Qumode fusion for continuous-variable cluster states

Jun Xin ⦿*

Department of Physics, Hangzhou Dianzi University, Hangzhou 310018, China

The quantum fusion technique enables the bonding of two cluster states together, and therefore provides a promising method to grow large-scale cluster states. Quantum fusion was first proposed in a discrete-variable regime. In terms of the resource usage, quantum fusion can be divided into two categories, which are type-I and type-II fusions. Type-I fusion consumes one qubit in the fusion procedure, while type-II consumes two qubits. However, for continuous-variable (CV) analogs, concrete schemes for realizing quantum fusions of cluster states with arbitrary topologies have not been shown yet. In this paper, we present the CV analog of quantum fusion schemes. We show that CV type-I fusion can be realized by an ancilla and two quantum nondemolition interactions, and CV type-II fusion can be realized by an entanglement swapping scheme. With finite squeezing considered, we analyze the extra errors added by the fusion procedures in CV cluster-state quantum computation. Our schemes are universal and can be generalized to fuse cluster states with arbitrary topologies.

I. INTRODUCTION

The cluster state, a specially prepared multipartite entangled state, provides the ability to perform one-way quantum computation (QC) [1]. To drive the cluster-state QC, quantum information is encoded onto the cluster and then is processed and read out by a sequence of local single-qubit projective measurements [2]. Due to the essential role of measurement, the cluster-state QC is inherently irreversible, and thus is called a one-way QC. Such cluster-state QC is promising because it constitutes a simplification over the standard circuit model of QC where unitary evolution and coherent control of individual qubits are required [3,4]. Due to its powerful application in QC, considerable efforts have been devoted to the study of the cluster state in recent decades [5–12].

While QC is typically performed in the discrete-variable (DV) regime, the continuous-variable (CV) cluster state shows distinct advantages over its discrete analog [13]. The main advantage is that the CV cluster state can be generated deterministically by using only off-line squeezed states and linear optics; this is in contrast to the DV linear-optics schemes, where the cluster states are created probabilistically. The CV cluster state can be efficiently described by mathematical graphs composed of a set of vertices and links. Two vertices are called neighbors if they are connected by a link. Each vertex represents one optical mode (qumode) of the cluster state, while the link stands for the interaction between two neighboring vertices. So far, various methods for generating a CV cluster state have been theoretically proposed [14–19] and experimentally realized [20–30].

Although CV cluster states are promising in QC, there are two outstanding challenges in realizing reliable, practical cluster-state QC. The first challenge is the computational errors caused by the finite squeezing of the CV cluster state, and the second one is the scalability.

In the practical implementation, the CV cluster state can never be perfect due to the finite squeezing of the initial modes in Gaussian cluster-state preparation. Such imperfection will give rise to extra quantum noise and thus the computational errors. However, it has been demonstrated that these errors can be corrected by a Gottesman-Kitaev-Preskill (GKP) qubit [31–33], which leads to a fault-tolerant cluster-state QC with a 15–17 dB squeezing threshold [34]. Recently, the GKP state has been successfully produced in superconducting resonators [35–37] and trapped-ion mechanical oscillators [38,39].

In addition to the computational errors, scalability is another important factor that should be considered for a CV cluster state. To meet computational universality, the CV cluster state must be of large scale and possess at least two-dimensional topology [27,28]. Given initial CV cluster states with small sizes and fixed topologies, quantum bonding techniques are necessary to bond them to become a larger one with any desired topology. In terms of the resource usage of qumodes (qubit in DV regime), there are three different types of bonding operations that are controlled-Z (CZ), type-I, and type-II fusion operations, respectively. The application scenarios of the above three bonding schemes are different, and all of them are of importance in the quantum bonding techniques. For two initial CV cluster states with qumodes $\{C_1, C_2, \ldots, C_n\}$ and $\{C'_1, C'_2, \ldots, C'_m\}$, the qumode sizes of the output cluster state after CZ, type-I fusion, and type-II fusion operations are $n + m$, $n + m - 1$, and $n + m - 2$, respectively. The CZ operation builds an interaction between any two qumodes C_i and C'_j of the two cluster states, and thus the sum of the qumode is unchanged. In the implementation, the CZ operation can be realized by using squeezing resources and linear optics [23]. Different from the CZ operation, type-I and type-II fusion operations consume one and two qumodes, respectively. Figure 1 shows an example of the action of type-I and type-II fusion operations. A fusion operation has its
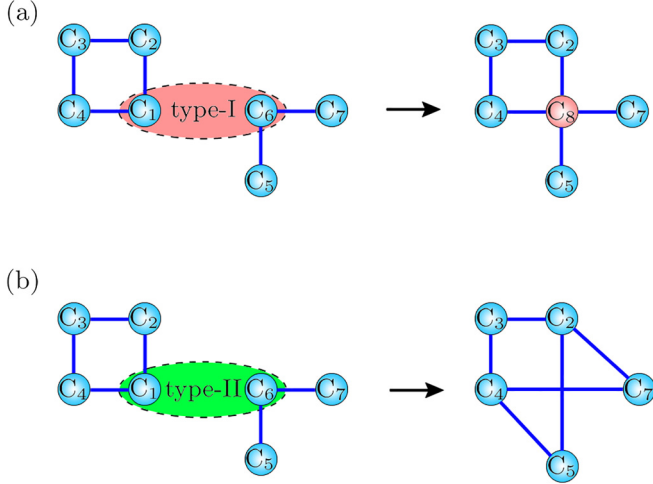
FIG. 1. Diagrammatic sketch of fusion operations between a four-mode square and three-mode linear cluster states. (a) Type-I fusion. (b) Type-II fusion.

unique advantages in constructing a cluster state with a large scale, compared to the method using CZ operations alone. For example, in Ref. [33] it has been shown that a type-II fusion gate with postselected measurement could prevent the error from propagating during the construction of a three-dimensional (3D) cluster state from finite-energy approximate GKP qubits; by contrast, the conventional method, which employs CZ gates alone to generate a 3D cluster state, yields more error probability. Thus, fusion operations are of great significance in scalable cluster-state QC. Type-I and type-II fusions of a cluster state were first proposed in Refs. [40] and [41] in the DV regime. For CV analogs, it has been pointed out that Gaussian projections are required to perform the qumode fusions for CV cluster states [42]. In addition, we also note that the entanglement swapping scheme can be used to realize the type-II fusion of two CV cluster states with some special topologies, such as line, square, and star shapes [43–45]. However, concrete schemes for realizing qumode fusions of CV cluster states with arbitrary topologies are still missing.

In this paper, we focus on the qumode fusion for CV cluster states. We show that a CV analog of type-I fusion can be realized by an ancilla squeezer and two quantum nondemolition (QND) interactions, while a CV analog of type-II fusion can be realized by an entanglement swapping scheme. Our results are universal and can be adequate to fuse CV clusters with arbitrary topologies. In addition, we also analyze the effect of finite squeezing on the extra errors added in the qumode fusion procedures in the cluster-state QC.

II. BACKGROUND OF CV CLUSTER STATE

An n-mode CV analog of an unweighted cluster state with qumodes $\{C_1, C_2, \ldots, C_n\}$ can be described by the nullifier operators given as $\hat{\sigma}_j = (\hat{p}_j^c - \sum_{k \in N_j} \hat{x}_k^c) \to 0$ ($j = 1, 2, \ldots, n$). Here, $\hat{x}_j^c$ and $\hat{p}_j^c$ are quadrature-amplitude and quadrature-phase operators of the qumode C_j. The qumode C_j is a vertex in the graph of the cluster state, and N_j denotes the index assemble of the vertices neighbored to C_j. The cluster

state requires that the variance of each nullifier approaches zero, in the limit of infinite squeezing. To prepare such a CV cluster, an alternative method is to employ squeezers and CZ gates [13]. We first prepare a set of quadrature-phase squeezed states denoted as $\hat{x}_j = e^r \hat{x}_j^{(0)}$ and $\hat{p}_j = e^{-r} \hat{p}_j^{(0)}$, where r is the squeezing degree and the superscript (0) denotes the vacuum mode. Then, we use CZ gates to build the links between the initially prepared squeezers, according to the graph of the desired cluster. The CZ gate, which corresponds to the operator $e^{i\hat{x}_j \otimes \hat{x}_k}$, transforms as

$$\hat{x}_j \to \hat{x}_j, \quad \hat{p}_j \to \hat{p}_j + \hat{x}_k,$$
$$\hat{x}_k \to \hat{x}_k, \quad \hat{p}_k \to \hat{p}_k + \hat{x}_j. \tag{1}$$

Therefore, an n-mode CV cluster state with arbitrary topology can be written as

$$\hat{x}_j^c = \hat{x}_j,$$
$$\hat{p}_j^c = \hat{p}_j + \sum_{k \in N_j} \hat{x}_k, \quad j = 1, 2, \ldots, n. \tag{2}$$

Obviously, such a cluster state satisfies the condition of the nullifier (i.e., $\hat{\sigma}_j \to 0$), when the squeezing degree is infinite. Note that a perfect CV cluster is unachievable in the practical implementation due to the finite squeezing. Finite-squeezing-induced errors will be accumulated in the cluster-state QC. However, these computational errors can be corrected by the GKP proposal [31,32], which is experimentally challenging but still achievable using current techniques [35–39]. In addition to the canonical method mentioned above using squeezing resources and CZ gates, a CV cluster state can also be produced using other schemes, such as linear-optics methods [15,20], single optical parametric oscillator methods [46,47], and temporal-mode encoding methods [27,28,48].

III. TYPE-I FUSION

A. Protocol

In the following, we show that a CV analog of type-I fusion can be realized by an ancilla squeezer and two QND interactions. Before introducing our scheme, we first give a brief introduction for the QND interaction. The QND interaction [49] is defined as $\hat{H}_{jk} = e^{i\hat{p}_j \otimes \hat{x}_k}$, which has the following transformations:

$$\hat{x}_j \to \hat{x}_j - \hat{x}_k, \quad \hat{p}_j \to \hat{p}_j,$$
$$\hat{x}_k \to \hat{x}_k, \quad \hat{p}_k \to \hat{p}_k + \hat{p}_j. \tag{3}$$

The QND interaction allows one to obtain sufficient information about one quadrature of the measured optical field, while still keeping this quadrature undisturbed. The efficiency of the QND interaction is dependent on the quantum resources that are employed, such as squeezing degree of the squeezers and the gain of parametric amplifiers [50]. An alternative method to realize the QND interaction is to use off-line squeezers, homodyne detectors, and feedforward modulations [51,52].

Now we consider the quantum bonding of two arbitrary CV clusters using a type-I fusion operation. The initial qumodes of the two clusters are denoted as $\{C_1, C_2, \ldots, C_n\}$

and $\{C_1^{\wr}, C_2^{\wr}, \ldots, C_m^{\wr}\}$, respectively. And their quadratures $\{\hat{x}_j^c, \hat{p}_j^c\}$ and $\{\hat{x}_k^{\wr c}, \hat{p}_k^{\wr c}\}$ yield the condition of a cluster state given in Eq. (2), respectively. In the type-I fusion procedure, we assume that the qumodes C_a and $C_b^{\wr}$ are fused together to become a new qumode denoted as C_A; the initial neighboring qumodes of C_a and $C_b^{\wr}$ becomes neighbored to the qumode C_A and the corresponding links are created [see Fig. 1(a) for a detailed example for the action of a type-I fusion operation]. In our scheme, two steps are required to realize the type-I fusion operation as mentioned above.

In step 1, we first prepare an ancilla squeezer C_A with its quadrature amplitude and quadrature phase denoted as $\hat{x}_A = e^r \hat{x}_A^{(0)}$ and $\hat{p}_A = e^{-r} \hat{p}_A^{(0)}$. Then, we entangle qumode C_A with C_a using the QND interaction $\hat{H}_{aA}$, which leads to the following transformations:

$$\hat{x}_a^c \to \hat{x}_a^c - \hat{x}_A = \hat{x}_a - \hat{x}_A, \quad (4)$$

$$\hat{p}_a^c \to \hat{p}_a^c = \hat{p}_a + \sum_{j \in N_a} \hat{x}_j, \quad (5)$$

$$\hat{x}_A \to \hat{x}_A, \quad (6)$$

$$\hat{p}_A \to \hat{p}_A + \hat{p}_a^c = \hat{p}_A + \hat{p}_a + \sum_{j \in N_a} \hat{x}_j. \quad (7)$$

Afterward, the output qumode C_a is sent to the homodyne detector to perform the feedforward modulations, which will be introduced in step 2. The other output qumode C_A is seeded into the second QND interaction $\hat{H}_{bA}$ combined with the qumode $C_b^{\wr}$, which leads to the following transformations:

$$\hat{x}_b^{\wr c} \to \hat{x}_b^{\wr c} - \hat{x}_A = \hat{x}_b^{\wr} - \hat{x}_A, \quad (8)$$

$$\hat{p}_b^{\wr c} \to \hat{p}_b^{\wr c} = \hat{p}_b^{\wr} + \sum_{k \in N_b} \hat{x}_k^{\wr}, \quad (9)$$

$$\hat{x}_A \to \hat{x}_A, \quad (10)$$

$$\hat{p}_A \to \hat{p}_A + \hat{p}_b^{\wr c} = \hat{p}_A + \hat{p}_a + \hat{p}_b^{\wr} + \sum_{j \in N_a} \hat{x}_j + \sum_{k \in N_b} \hat{x}_k^{\wr}. \quad (11)$$

At the end of step 1, we achieve three output modes C_a, $C_b^{\wr}$, and C_A, and their quadratures are given by Eqs. (4), (5), and (8)–(11).

In step 2, we employ homodyne detection to measure the quadrature amplitude $\hat{x}_a^c$ ($\hat{x}_b^{\wr c}$) of the mode C_a ($C_b^{\wr}$). The measurement outcome of the observable $\hat{x}_a^c$ is fed forward to each neighboring qumode of C_a as a displacement operation, $\exp[-i\hat{x}_a^c \otimes \hat{x}_{N_a(l)}^c]$. Here, $\hat{x}_{N_a(l)}^c$ is the quadrature amplitude of the qumode $C_{N_a(l)}$, and $C_{N_a(l)}$ is the lth neighboring qumode of C_a ($l = 1, 2, \ldots, \varepsilon_a$), with ε_a being the number of corresponding neighbors. Note that similar feedforward modulation is also performed on each neighboring qumode of $C_b^{\wr}$. The quadratures of each qumode $C_{N_a(l)}$ can be written as

$$\hat{x}_{N_a(l)}^c = \hat{x}_{N_a(l)},$$
$$\hat{p}_{N_a(l)}^c = \hat{p}_{N_a(l)} + \sum_{j \in N_{N_a(l)}} \hat{x}_j, \quad l = 1, 2, \ldots, \varepsilon_a, \quad (12)$$

where $N_{N_a(k)}$ denotes the index assemble of the qumodes neighbored to $C_{N_a(l)}$. These quadratures yield the following transformations after the displacement operation:

$$\hat{x}_{N_a(l)}^c \to \hat{x}_{N_a(l)}^c = \hat{x}_{N_a(l)},$$
$$\hat{p}_{N_a(l)}^c \to \hat{p}_{N_a(l)}^c - \hat{x}_a^c$$
$$= \hat{p}_{N_a(l)} + \hat{x}_A - \hat{x}_a + \sum_{j \in N_{N_a(l)}} \hat{x}_j$$
$$= \hat{p}_{N_a(l)} + \sum_{j \in N_{N_a(l)}^{[a \to A]}} \hat{x}_j, \quad l = 1, 2, \ldots, \varepsilon_a, \quad (13)$$

where $N_{N_a(l)}^{[a \to A]} \equiv [N_{N_a(l)} \backslash a] \cup A$ indicates the index assemble $N_{N_a(l)}$ with its element a replaced with A. In the derivation of Eq. (13), we have used the fact that $a \in N_{N_a(l)}$ because the qumodes $C_{N_a(l)}$ and C_a are adjacent. Similar to the feedforward scheme as mentioned above, we use the measurement outcome of the observable $\hat{x}_b^{\wr c}$ to modulate the neighboring qumodes of $C_b^{\wr}$. The mth neighboring qumode $C_{N_b(m)}^{\wr}$ follows the transformations as

$$\hat{x}_{N_b(m)}^{\wr c} \to \hat{x}_{N_b(m)}^{\wr c} = \hat{x}_{N_b(m)},$$
$$\hat{p}_{N_b(m)}^{\wr c} \to \hat{p}_{N_b(m)}^{\wr c} - \hat{x}_b^{\wr c}$$
$$= \hat{p}_{N_b(m)}^{\wr} + \sum_{k \in N_{N_b(m)}^{[b \to A]}} \hat{x}_k, \quad m = 1, 2, \ldots, \varepsilon_b, \quad (14)$$

where ε_b is the number of the neighboring qumodes of $C_b^{\wr}$.

Now let us see the actions of the two steps as discussed above. First, there are two qumodes C_a and $C_b^{\wr}$ consumed in the fusion procedure. Meanwhile, a new qumode C_A is inserted into the cluster state, and its quadratures are given by Eqs. (10) and (11). It can be simply found that the qumode C_A is linked to all the qumodes $\{C_{N_a(1)}, C_{N_a(2)}, \ldots, C_{N_a(\varepsilon_a)}\}$ and $\{C_{N_b(1)}^{\wr}, C_{N_b(2)}^{\wr}, \ldots, C_{N_b(\varepsilon_b)}^{\wr}\}$ that are initially neighbored to C_a and $C_b^{\wr}$, respectively. From the perspective of these neighboring qumodes $C_{N_a(l)}$ and $C_{N_b(m)}^{\wr}$ as shown in Eqs. (13) and (14), their links connected with C_a and $C_b^{\wr}$ are cut off, and all of them become neighbored to the qumode C_A, after the fusion procedure. In addition, the variance of each nullifier $\hat{\sigma}_j$ approaches zero in the limit of infinite squeezing, where $j = N_a(1), N_a(2), \ldots, N_a(\varepsilon_a), N_b(1), N_b(2), \ldots, N_b(\varepsilon_b)$ and A. Therefore, the type-I fusion of two CV cluster states $\{C_1, C_2, \ldots, C_n\}$ and $\{C_1^{\wr}, C_2^{\wr}, \ldots, C_m^{\wr}\}$ is realized. Note that in the above discussions, we make no special assumptions about the topologies of the initial clusters, as well as the fusion qumodes C_a and $C_b^{\wr}$. Thus, our scheme is universal and thus can be generalized to perform a type-I fusion operation for arbitrary CV cluster states.

B. Error analysis

In the above discussions, we have shown that the type-I fusion for CV cluster states can be realized by using an ancilla squeezer and two QND interactions. However, our discussions are based on the infinite squeezing, which is unachievable in real practice. The finite-squeezing-induced errors can affect the efficiency of cluster-state QC [15], and therefore should
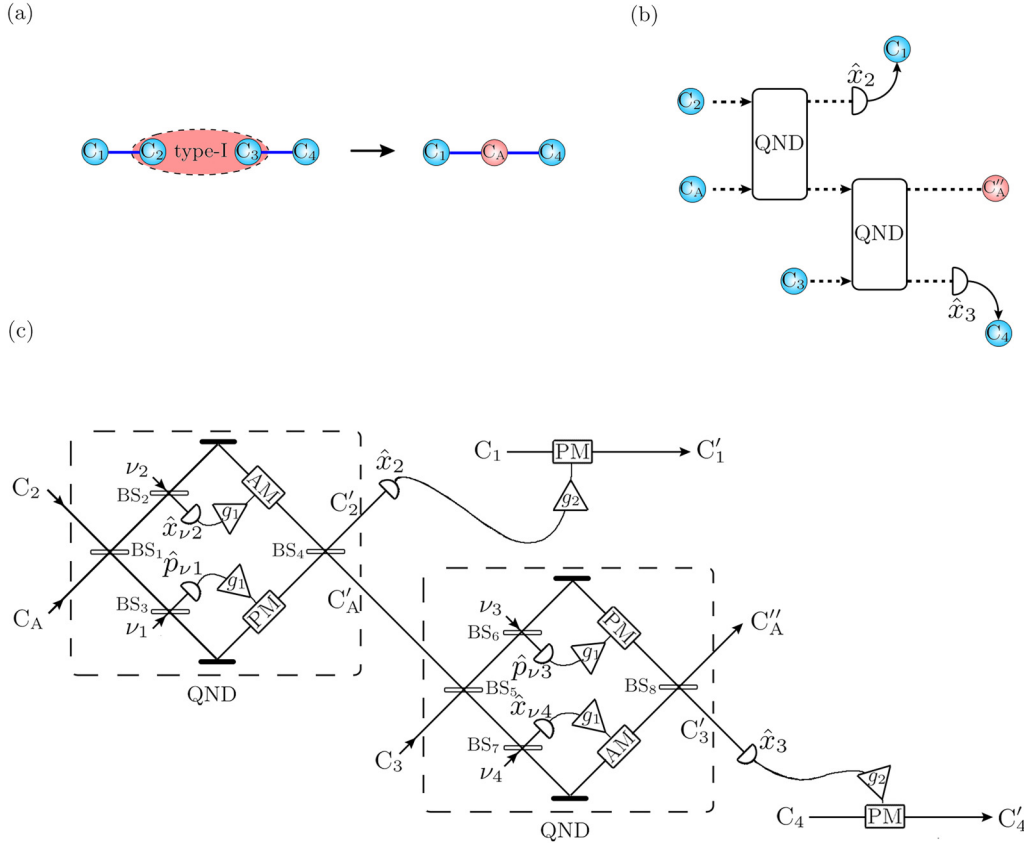
FIG. 2. CV analog of type-I fusion between two two-mode cluster states. (a) Action of type-I fusion. (b) Diagrammatic sketch of type-I fusion scheme using an ancilla squeezer and two QND interactions. (c) Detailed experimental scenario. ν_1 and ν_3: quadrature-amplitude squeezed modes; ν_2 and ν_4: quadrature-phase squeezed modes; AM: amplitude modulation; PM: phase modulation. The transmissivities of the beam splitters $\{BS_1, BS_5\}$, $\{BS_4, BS_8\}$, and $\{BS_2, BS_3, BS_6, BS_7\}$ are $1/(1+T)$, $T/(1+T)$, and T.

be considered. In this section, we will analyze the effect of finite squeezing on our CV analog of a type-I fusion scheme. We find that the extra noise added by our type-I fusion scheme consists of two parts. The first part comes from the two qumodes (i.e., the qumodes C_a and C_b' in Sec. III A) that are to be fused together in the fusion procedure. The second part comes from the squeezers employed in the QND interactions. For a better understanding, in what follows we consider a simple example as shown in Fig. 2(a), where two two-mode clusters are fused together. The diagrammatic sketch of the corresponding type-I fusion scheme and its detailed experimental scenario are shown in Figs. 2(b) and 2(c), respectively. Our error model can also be extended to the fusion of cluster states with any other topologies.

It is well known that the efficiency of the QND interactions is dependent on the squeezing resources that are employed. Finite squeezing will unavoidably give rise to extra noise in the QND interaction and thus degrade the efficiency of our type-I fusion scheme. Using the QND interaction proposed in Ref. [51], we show our type-I fusion scheme in Fig. 2 with a detailed example considered. For two two-mode cluster states denoted as $\{C_1, C_2\}$ and $\{C_3, C_4\}$, our goal is to realize the type-I fusion of them by fusing the qumodes C_2 and C_3 together to become a new qumode C_A. As shown by the

dashed boxes in Fig. 2(c), each QND interaction introduces two squeezers, i.e., the two modes ν_1 and ν_2 for the first QND, and the two modes ν_3 and ν_4 for the second QND. Here, we assume that the modes ν_1 and ν_3 are quadrature-amplitude squeezed, and the modes ν_2 and ν_4 are quadrature-phase squeezed. Their quadratures are denoted as $\hat{x}_{\nu 1} = e^{-r}\hat{x}_{\nu 1}^{(0)}$, $\hat{p}_{\nu 1} = e^r\hat{p}_{\nu 1}^{(0)}$, $\hat{x}_{\nu 3} = e^{-r}\hat{x}_{\nu 3}^{(0)}$, $\hat{p}_{\nu 3} = e^r\hat{p}_{\nu 3}^{(0)}$, $\hat{x}_{\nu 2} = e^r\hat{x}_{\nu 2}^{(0)}$, $\hat{p}_{\nu 2} = e^{-r}\hat{p}_{\nu 2}^{(0)}$, $\hat{x}_{\nu 4} = e^r\hat{x}_{\nu 4}^{(0)}$, and $\hat{p}_{\nu 4} = e^{-r}\hat{p}_{\nu 4}^{(0)}$, respectively.

Now we follow the type-I fusion scheme as discussed in Sec. III A. To perform the first QND interaction as shown by the left dashed box in Fig. 2(c), we first mix the qumode C_2 and an ancilla squeezer C_A on a linear beam splitter BS_1 with transmissivity $1/(1+T)$. Afterward, the mode C_2 (C_A) is coupled with the squeezer ν_1 (ν_2) using another beam splitter BS_3 (BS_2) with transmissivity T. After the linear coupling, the quadrature phase (quadrature amplitude) of the squeezer ν_1 (ν_2) is measured by a homodyne detector. The measurement outcomes of the observable $\hat{p}_{\nu 1}$ ($\hat{x}_{\nu 2}$) are then fed forward to the qumode ν_1 (ν_2) using phase (amplitude) modulation with gain of $g_1 = -\sqrt{(1-T)/T}$. After this postcorrection procedure, the qumodes C_2 and C_A are mixed again on a beam splitter BS_4 with transmissivity $T/(1+T)$, and their corresponding output qumodes are denoted as C_2' and C_A'. The input-output relationship of the first QND interaction is given

by

$$\hat{x}'_2 = \hat{x}^c_2 - \left(\frac{1}{\sqrt{T}} - \sqrt{T}\right)\hat{x}_A + \frac{\sqrt{T}\sqrt{1-T}}{\sqrt{1+T}}\hat{x}_{\nu 1},$$

$$\hat{p}'_2 = \hat{p}^c_2 - \frac{\sqrt{1-T}}{\sqrt{1+T}}\hat{p}_{\nu 2},$$

$$\hat{x}'_A = \hat{x}_A + \frac{\sqrt{1-T}}{\sqrt{1+T}}\hat{x}_{\nu 1},$$

$$\hat{p}'_A = \hat{p}_A + \left(\frac{1}{\sqrt{T}} - \sqrt{T}\right)\hat{p}^c_2 + \frac{\sqrt{T}\sqrt{1-T}}{\sqrt{1+T}}\hat{p}_{\nu 2}. \quad (15)$$

By adjusting the parameter T, the above transformations can be equivalent to the QND interaction as given in Eqs. (4)–(7), but with extra noise added into each quadrature. When the initial squeezers ν_1 and ν_2 are of finite squeezing, the errors caused by such extra noise will be accumulated in the following steps of the type-I fusion procedure. After the first QND interaction, we couple the modes C_3 and C'_A using the second QND interaction, and their corresponding outputs are denoted as C'_3 and C''_A, respectively. In the end of the type-I fusion, the quadrature amplitude of the modes C'_2 and C'_3 is measured by homodyne detectors, respectively; the measurement outcomes of the observables $\hat{x}_2$ and $\hat{x}_3$ are fed forward to the modes C_1 and C_4 using phase modulation with gain of $g_2 = 1$. The output state from the type-I fusion is given by

$$\hat{x}''_A = \hat{x}_A + \frac{\sqrt{1-T}}{\sqrt{1+T}}(\hat{x}_{\nu 1} + \hat{x}_{\nu 3}),$$

$$\hat{p}''_A = \hat{p}_A + \left(\frac{1}{\sqrt{T}} - \sqrt{T}\right)(\hat{p}_2 + \hat{p}_3 + \hat{x}_1 + \hat{x}_4) + \frac{\sqrt{T}\sqrt{1-T}}{\sqrt{1+T}}(\hat{p}_{\nu 2} + \hat{p}_{\nu 4}),$$

$$\hat{x}'_1 = \hat{x}_1,$$

$$\hat{p}'_1 = \hat{p}_1 + \left(\frac{1}{\sqrt{T}} - \sqrt{T}\right)\hat{x}_A - \frac{\sqrt{T}\sqrt{1-T}}{\sqrt{1+T}}\hat{x}_{\nu 1},$$

$$\hat{x}'_4 = \hat{x}_4,$$

$$\hat{p}'_4 = \hat{p}_4 + \left(\frac{1}{\sqrt{T}} - \sqrt{T}\right)\hat{x}_A + \frac{(1-T)^{\frac{3}{2}}}{\sqrt{T}\sqrt{1+T}}\hat{x}_{\nu 1} - \frac{\sqrt{T}\sqrt{1-T}}{\sqrt{1+T}}\hat{x}_{\nu 3}. \quad (16)$$

Obviously, the two initial two-mode cluster states $\{C_1, C_2\}$ and $\{C_3, C_4\}$ have now been fused together to become a three-mode linear cluster state $\{C'_1, C''_A, C'_4\}$ after our type-I fusion scheme. Meanwhile, extra noise is added. In the following, we analyze the finite-squeezing-induced errors in the cluster-state QC.

A single-qubit teleportation circuit lies at the heart of the cluster-state QC [13]. For the CV analog, here we consider the quantum teleportation of an unknown single-mode quantum state through the cluster state generated by our type-I fusion scheme. Using the linear cluster state $\{C'_1, C''_A, C'_4\}$, an unknown input mode (its quadratures are denoted as $\hat{x}_{in}$ and $\hat{p}_{in}$) is teleported from the qumode C'_1 to C'_4. To perform such teleportation, the input mode is first coupled with the qumode C'_1 using the CZ gate $e^{i\hat{x}_{in} \otimes \hat{x}'_1}$, which yields the transformations in Eq. (1). Then, quadrature-phase measurements are performed on the input mode and two qumodes C'_1 and C''_A, and the corresponding results are denoted as s_{in}, s_1 and s_A. These measurement outcomes are used to perform the postcorrection procedure, and the corresponding correction operation is given by $\hat{X}_A(-\xi s_{in})\hat{X}_4(-s_1)\hat{Z}_4(-\xi^{-1}s_A)\hat{F}_4^\dagger$. Here, the displacement operators $\hat{X}_j(s_k) = e^{is_k\hat{x}_j}$ and $\hat{Z}_j(s_k) = e^{-is_k\hat{p}_j}$ yield the transformations that $\hat{X}_j^\dagger(s_k)\hat{x}_j\hat{X}_j(s_k) = \hat{x}_j$, $\hat{X}_j^\dagger(s_k)\hat{p}_j\hat{X}_j(s_k) = \hat{p}_j + s_k$, $\hat{Z}_j^\dagger(s_k)\hat{x}_j\hat{Z}_j(s_k) = \hat{x}_j + s_k$, $\hat{Z}_j^\dagger(s_k)\hat{p}_j\hat{Z}_j(s_k) = \hat{p}_j$, and $\xi = (1-T)/$

$\sqrt{T}$. The inverse Fourier transform operator $\hat{F}_j^\dagger$ transforms as $\hat{x}_j \to \hat{p}_j$ and $\hat{p}_j \to -\hat{x}_j$, i.e., $-\pi/2$ rotation in phase space. After the above postcorrection procedure, the qumode C'_4 becomes

$$\hat{x}'_4 \to \hat{x}_{in} + \hat{p}_1 - \hat{p}_4 - \frac{\sqrt{1-T}}{\sqrt{T}\sqrt{1+T}}\hat{x}_{\nu 1} + \frac{\sqrt{T}\sqrt{1-T}}{\sqrt{1+T}}\hat{x}_{\nu 3},$$

$$\hat{p}'_4 \to \hat{p}_{in} - \hat{p}_2 - \hat{p}_3 - \frac{\sqrt{T}}{1-T}\hat{p}_A - \frac{T}{\sqrt{1-T^2}}(\hat{p}_{\nu 2} + \hat{p}_{\nu 4}). \quad (17)$$

In the above derivation, we have used the fact that the displacement operators $\hat{X}_j(s_k)$ and $\hat{Z}_j(s_k)$ are equivalent to the controlled-logical gate operators $\hat{X}_j(\hat{p}_k)$ and $\hat{Z}_j(\hat{p}_k)$. This is because the feedforward circuit, i.e., executing displacement after measurement, is equivalent to the circuit where the measurement is performed after a controlled-logical gate.

To study the extra noise added by our type-I fusion scheme, we consider employing a standard three-mode linear cluster $\{C_1, C_A, C_4\}$, which yields the cluster condition in Eq. (2), to perform the quantum teleportation. Using a similar method as we have discussed in the derivation of Eq. (17), it can be simply demonstrated that the output quadratures of the quantum teleportation through a standard three-mode linear

cluster state are given by

$$\hat{x}_4^c \rightarrow \hat{x}_{\text{in}} + \hat{p}_1 - \hat{p}_4,$$
$$\hat{p}_4^c \rightarrow \hat{p}_{\text{in}} - \hat{p}_A. \tag{18}$$

By comparing Eq. (17) with Eq. (18), it can be found that the extra noise added by our type-I fusion scheme comes from two parts. The first part is the two qumodes C_2 and C_3. In our scheme, these two qumodes are detected, and the measurement results are fed forward to the qumodes C_1 and C_4. In this postcorrection procedure, the quadrature phase $\hat{p}_2$ and $\hat{p}_3$ cannot be canceled, which gives rise to finite-squeezing-induced noise of $2e^{-2r}$ in $\hat{p}_4'$. The second part is the squeezers $v1, v2, \ldots, v4$, which are employed in the QND interactions. The extra noise added by these squeezers is $e^{-2r}(1-T)(1+T^2)/[T(1+T)]$ in $\hat{x}_4'$ and $2e^{-2r}T^2/(1-T^2)$ in $\hat{p}_4'$. In addition, we also note that $\hat{p}_A$ is scaled as $\sqrt{T}/(1-T)$ in Eq. (17). Considering a unity-gain case where $T = (3 - \sqrt{5})/2$, the extra noise added by our type-I fusion scheme is $3e^{-2r}/\sqrt{5}$ in $\hat{x}_4'$ and $e^{-2r}(5 + 3\sqrt{5})/5$ in $\hat{p}_4'$. Note that the above error analysis can be extended to the type-I fusion of cluster states with arbitrary topologies. We find that for any two cluster states, the sum of the extra noise added to both the quadrature amplitude and quadrature phase by our type-I fusion scheme is $e^{-2r}(6 + \sqrt{5})/\sqrt{5}$ in the unity-gain case.

IV. TYPE-II FUSION

Different from the type-I fusion operation, type-II fusion of two cluster states consumes two qumodes. For two cluster states $\{C_1, C_2, \ldots, C_n\}$ and $\{C_1^\lambda, C_2^\lambda, \ldots, C_m^\lambda\}$, we assume that the qumodes C_a and C_b^λ are to be fused together. Type-II fusion requires that both of these qumodes are removed from the output cluster state. Meanwhile, each neighbor of the qumode C_a becomes neighbored to all the neighboring qumodes of C_b^λ, and vice versa. Note that in some special cases, the type-II fusion scheme can replace type-I fusion, but with some extra operations involved. Take the case shown in Fig. 2(a) as an example. To realize the type-I fusion operation between two two-mode cluster states, we can first use a type-II fusion scheme to bond the qumodes C_1 and C_4. Afterward, we cut off the bonding with the help of the bond erasing operation [53], and then use CZ operations to build new bonds between the qumodes C_1, C_4 and an ancillary mode C_A. In Ref. [44], it has been shown that the CV analog of type-II fusion can be realized by an entanglement swapping scheme. However, the type-II fusion scheme is only focused on the cluster states with some special topologies, such as line-, square- and star-shape clusters. A general description of a CV analog of type-II fusion between two cluster states with arbitrary topologies has not been shown yet. In this section, we will solve this issue. For simplification, we omit the mathematical forms of the initial qumodes of C_a and C_b^λ, as well as their neighboring qumodes in the following discussions, which can be referred to in Eqs. (2) and (12).

To realize the CV analog of type-II fusion, two steps are required. In step 1, we first apply an inverse Fourier transformation on the qumode C_b^λ, which transforms as $\hat{x}_b^{\lambda c} \rightarrow \hat{p}_b^{\lambda c}$ and $\hat{p}_b^{\lambda c} \rightarrow -\hat{x}_b^{\lambda c}$. Afterward, the qumodes C_a and C_b^λ are mixed

onto a balanced beam splitter, leading to the following transformations:

$$\hat{x}_a^c \rightarrow \frac{1}{\sqrt{2}} \left(\hat{x}_a - \hat{p}_b^\lambda - \sum_{k \in N_b} \hat{x}_k^\lambda \right),$$

$$\hat{p}_a^c \rightarrow \frac{1}{\sqrt{2}} \left(\hat{p}_a + \sum_{j \in N_a} \hat{x}_j + \hat{x}_b^\lambda \right),$$

$$\hat{x}_b^{\lambda c} \rightarrow \frac{1}{\sqrt{2}} \left(-\hat{x}_a - \hat{p}_b^\lambda - \sum_{k \in N_b} \hat{x}_k^\lambda \right),$$

$$\hat{p}_b^{\lambda c} \rightarrow \frac{1}{\sqrt{2}} \left(-\hat{p}_a - \sum_{j \in N_a} \hat{x}_j + \hat{x}_b^\lambda \right). \tag{19}$$

In step 2, we employ homodyne detectors to measure the quadrature amplitude $\hat{x}_a^c$ of the qumode C_a and the quadrature phase $\hat{p}_b^{\lambda c}$ of the qumode C_b^λ, and the corresponding results are denoted as s_a and s_b, respectively. Afterward, the measurement outcome s_a (s_b) is fed forward to each neighboring qumode of C_a (C_b^λ) using phase modulation with gain of $\sqrt{2}$. The corresponding feedforward modulations transform as

$$\hat{x}_{N_a(l)}^c \rightarrow \hat{x}_{N_a(l)}^c = \hat{x}_{N_a(l)},$$

$$\hat{p}_{N_a(l)}^c \rightarrow \hat{p}_{N_a(l)}^c - \hat{x}_a^c = \hat{p}_{N_a(l)} + \hat{p}_b^\lambda + \sum_{j \in N_{N_a(l)}^{[a \rightarrow N_b]}} \hat{x}_j,$$

$$\hat{x}_{N_b(m)}^{\lambda c} \rightarrow \hat{x}_{N_b(m)}^{\lambda c} = \hat{x}_{N_b(m)},$$

$$\hat{p}_{N_b(m)}^{\lambda c} \rightarrow \hat{p}_{N_b(m)}^{\lambda c} - \hat{p}_b^{\lambda c} = \hat{p}_{N_b(m)}^\lambda + \hat{p}_a + \sum_{k \in N_{N_b(m)}^{[b \rightarrow N_a]}} \hat{x}_k^\lambda, \tag{20}$$

where $l = 1, 2, \ldots, \varepsilon_a$ and $k = 1, 2, \ldots, \varepsilon_b$, ε_a in which ε_b denote the number of the neighboring qumodes of C_a and C_b.

As shown in Eq. (20), the two cluster states $\{C_1, C_2, \ldots, C_n\}$ and $\{C_1^\lambda, C_2^\lambda, \ldots, C_m^\lambda\}$ have now been fused together by the entanglement swapping scheme, which is of the topology as follows. First, the links between the qumode C_a (as well as C_b) and its neighboring qumodes are cut off. The qumodes C_a and C_b are removed from the cluster state. Second, each neighboring qumode of C_a becomes neighbored to all the neighboring qumodes of C_b, and vice versa. Therefore, type-II fusion of the CV clusters is realized.

Considering the finite squeezing case, the extra noise added by the CV analog of type-II fusion is caused by the two qumodes C_a and C_b. As seen in Eq. (20), an extra term $\hat{p}_b^\lambda$ ($\hat{p}_a$) is added in $\hat{p}_{N_a(l)}^c$ ($\hat{p}_{N_b(m)}^{\lambda c}$). To teleport an unknown single-mode quantum state using the cluster state generated from the type-II fusion scheme, it can be simply demonstrated that extra noise of e^{-2r} will be added in both the quadrature amplitude and quadrature phase of the output mode.

In addition, the CV analog of type-II fusion can also be applied to construct a 3D cluster state based on finite-energy approximate GKP encodings [33,45]. It has been shown that the error probability in generating a 3D cluster state results from two independent errors, where one error originates from the GKP qubit itself and the second error occurs during the

fusion gates. Comparing with the conventional method in generating a 3D cluster state which only uses CZ gates between neighboring nodes, it has been shown that a fusion gate with postselected measurement can efficiently avoid the accumulation of errors during the construction process of a 3D cluster state at the price of determinacy, and therefore relaxes the squeezing level required by the fault-tolerant QC.

V. CONCLUSION

In summary, quantum fusion is of great significance in cluster-state QC. It bonds two cluster states together to become a larger one, and therefore improves the scalability of the quantum network based on a cluster state. In terms of the resource usage, there are two types of quantum fusion operations, which are type-I and type-II fusions. In the DV regime, the qubits' fusion schemes have been proposed in Refs. [40,41] using nondeterministic gates. However, concrete schemes for realizing qumode fusions of CV cluster states with arbitrary topologies have not been shown yet. In this paper, we have solved this issue. We have demonstrated that the CV analog of type-I fusion can be realized by an ancilla squeezer and two QND interactions, and the type-II fusion can be realized by an entanglement swapping scheme. We have also analyzed the finite-squeezing-induced errors added by the quantum fusion operations in a CV cluster-state QC. The CV analog of quantum fusion schemes, as well as their error models, presented in this paper can be generalized to the cluster states with arbitrary topologies. Our results may pave the way to construct large-scale CV cluster states in practice.

[1] R. Raussendorf and H. J. Briegel, Phys. Rev. Lett. **86**, 5188 (2001).

[2] P. Walther, K. J. Resch, T. Rudolph, E. Schenck, H. Weinfurter, V. Vedral, M. Aspelmeyer, and A. Zeilinger, Nature (London) **434**, 169 (2005).

[3] R. Raussendorf, D. E. Browne, and H. J. Briegel, Phys. Rev. A **68**, 022312 (2003).

[4] N. C. Menicucci, Phys. Rev. A **83**, 062314 (2011).

[5] T. C. Ralph, A. J. F. Hayes, and A. Gilchrist, Phys. Rev. Lett. **95**, 100501 (2005).

[6] M. Varnava, D. E. Browne, and T. Rudolph, Phys. Rev. Lett. **97**, 120501 (2006).

[7] C.-Y. Lu, X.-Q. Zhou, O. Gühne, W.-B. Gao, J. Zhang, Z.-S. Yuan, A. Goebel, T. Yang, and J.-W. Pan, Nat. Phys. **3**, 91 (2007).

[8] K. Chen, C.-M. Li, Q. Zhang, Y.-A. Chen, A. Goebel, S. Chen, A. Mair, and J.-W. Pan, Phys. Rev. Lett. **99**, 120503 (2007).

[9] T. Tanamoto, Y.-X. Liu, X. Hu, and F. Nori, Phys. Rev. Lett. **102**, 100501 (2009).

[10] M. Lanyon, Benjamin P.and Barbieri, M. P. Almeida, T. Jennewein, T. C. Ralph, K. J. Resch, G. J. Pryde, J. L. O'Brien, A. Gilchrist, and A. G. White, Nat. Phys. **5**, 134 (2009).

[11] I. Schwartz, D. Cogan, E. R. Schmidgall, Y. Don, L. Gantz, O. Kenneth, N. H. Lindner, and D. Gershoni, Science **354**, 434 (2016).

[12] M. Pant, D. Towsley, D. Englund, and S. Guha, Nat. Commun. **10**, 1070 (2019).

[13] N. C. Menicucci, P. van Loock, M. Gu, C. Weedbrook, T. C. Ralph, and M. A. Nielsen, Phys. Rev. Lett. **97**, 110501 (2006).

[14] J. Zhang and S. L. Braunstein, Phys. Rev. A **73**, 032318 (2006).

[15] P. van Loock, C. Weedbrook, and M. Gu, Phys. Rev. A **76**, 032321 (2007).

[16] J. Zhang, Phys. Rev. A **78**, 034301 (2008).

[17] A. Tan, C. Xie, and K. Peng, Phys. Rev. A **79**, 042338 (2009).

[18] Y. Cai, J. Feng, H. Wang, G. Ferrini, X. Xu, J. Jing, and N. Treps, Phys. Rev. A **91**, 013843 (2015).

[19] S. Yokoyama, R. Ukai, S. C. Armstrong, J.-I. Yoshikawa, P. van Loock, and A. Furusawa, Phys. Rev. A **92**, 032304 (2015).

[20] X. Su, A. Tan, X. Jia, J. Zhang, C. Xie, and K. Peng, Phys. Rev. Lett. **98**, 070502 (2007).

[21] M. Yukawa, R. Ukai, P. van Loock, and A. Furusawa, Phys. Rev. A **78**, 012301 (2008).

[22] R. Ukai, N. Iwata, Y. Shimokawa, S. C. Armstrong, A. Politi, J.-I. Yoshikawa, P. van Loock, and A. Furusawa, Phys. Rev. Lett. **106**, 240504 (2011).

[23] R. Ukai, S. Yokoyama, J.-i. Yoshikawa, P. van Loock, and A. Furusawa, Phys. Rev. Lett. **107**, 250501 (2011).

[24] X. Su, Y. Zhao, S. Hao, X. Jia, C. Xie, and K. Peng, Opt. Lett. **37**, 5178 (2012).

[25] S. Yokoyama, R. Ukai, S. C. Armstrong, C. Sornphiphatphong, T. Kaji, S. Suzuki, J.-I. Yoshikawa, H. Yonezawa, N. C. Menicucci, and A. Furusawa, Nat. Photon. **7**, 982 (2013).

[26] J.-i. Yoshikawa, S. Yokoyama, T. Kaji, C. Sornphiphatphong, Y. Shiozawa, K. Makino, and A. Furusawa, APL Photon. **1**, 060801 (2016).

[27] W. Asavanant, Y. Shiozawa, S. Yokoyama, B. Charoensombutamon, H. Emura, R. N. Alexander, S. Takeda, J.-I. Yoshikawa, N. C. Menicucci, H. Yonezawa, and A. Furusawa, Science **366**, 373 (2019).

[28] M. V. Larsen, X. Guo, C. R. Breum, J. S. Neergaard-Nielsen, and U. L. Andersen, Science **366**, 369 (2019).

[29] W. Asavanant, B. Charoensombutamon, S. Yokoyama, T. Ebihara, T. Nakamura, R. N. Alexander, M. Endo, J.-I. Yoshikawa, N. C. Menicucci, H. Yonezawa, and A. Furusawa, Phys. Rev. Appl. **16**, 034005 (2021).

[30] M. V. Larsen, X. Guo, C. R. Breum, J. S. Neergaard-Nielsen, and U. L. Andersen, Nat. Phys. **17**, 1018 (2021).

[31] D. Gottesman, A. Kitaev, and J. Preskill, Phys. Rev. A **64**, 012310 (2001).

[32] N. C. Menicucci, Phys. Rev. Lett. **112**, 120504 (2014).

[33] K. Fukui, A. Tomita, A. Okamoto, and K. Fujii, Phys. Rev. X **8**, 021054 (2018).

[34] B. W. Walshe, L. J. Mensen, B. Q. Baragiola, and N. C. Menicucci, Phys. Rev. A **100**, 010301(R) (2019).

[35] N. Ofek, A. Petrenko, R. Heeres, P. Reinhold, Z. Leghtas, B. Vlastakis, Y. Liu, L. Frunzio, S. M. Girvin, L. Jiang, M. Mirrahimi, M. H. Devoret, and R. J. Schoelkopf, Nature (London) **536**, 441 (2016).

[36] R. W. Heeres, P. Reinhold, N. Ofek, L. Frunzio, L. Jiang, M. H. Devoret, and R. J. Schoelkopf, Nat. Commun. **8**, 94 (2017).

[37] P. Campagne-Ibarcq, A. Eickbusch, S. Touzard, E. Zalys-Geller, N. E. Frattini, V. V. Sivak, P. Reinhold, S. Puri, S. Shankar, R. J. Schoelkopf, L. Frunzio, M. Mirrahimi, and M. H. Devoret, Nature (London) **584**, 368 (2020).

[38] C. Flühmann, T. L. Nguyen, M. Marinelli, V. Negnevitsky, K. Mehta, and J. P. Home, Nature (London) **566**, 513 (2019).

[39] B. de Neeve, T.-L. Nguyen, T. Behrle, and J. P. Home, Nat. Phys. **18**, 296 (2022).

[40] F. Verstraete and J. I. Cirac, Phys. Rev. A **70**, 060302(R) (2004).

[41] D. E. Browne and T. Rudolph, Phys. Rev. Lett. **95**, 010501 (2005).

[42] M. Ohliger, K. Kieling, and J. Eisert, Phys. Rev. A **82**, 042336 (2010).

[43] X. Su, C. Tian, X. Deng, Q. Li, C. Xie, and K. Peng, Phys. Rev. Lett. **117**, 240503 (2016).

[44] C. Tian, D. Han, Y. Wang, and X. Su, Opt. Express **26**, 29159 (2018).

[45] K. P. Seshadreesan, P. Dhara, A. Patil, L. Jiang, and S. Guha, Phys. Rev. A **105**, 052416 (2022).

[46] N. C. Menicucci, S. T. Flammia, and O. Pfister, Phys. Rev. Lett. **101**, 130501 (2008).

[47] X. Zhu, C.-H. Chang, C. González-Arciniegas, A. Pe'er, J. Higgins, and O. Pfister, Optica **8**, 281 (2021).

[48] N. C. Menicucci, X. Ma, and T. C. Ralph, Phys. Rev. Lett. **104**, 250503 (2010).

[49] M. F. Bocko and R. Onofrio, Rev. Mod. Phys. **68**, 755 (1996).

[50] B. Yurke, J. Opt. Soc. Am. B **2**, 732 (1985).

[51] R. Filip, P. Marek, and U. L. Andersen, Phys. Rev. A **71**, 042308 (2005).

[52] J.-i. Yoshikawa, Y. Miwa, A. Huck, U. L. Andersen, P. van Loock, and A. Furusawa, Phys. Rev. Lett. **101**, 250501 (2008).

[53] R. Filip, Phys. Rev. A **67**, 042111 (2003).